

Feeder-Cell Ingestion of Seeding Aerosol from Cloud Base Determined by Tracking Radar Chaff

ROGER F. REINKING AND BROOKS E. MARTNER

NOAA/ERL/Environmental Technology Laboratory, Boulder, Colorado

(Manuscript received 7 November 1994, in final form 16 May 1995)

ABSTRACT

Questions of delivery, transport, and dispersion of cloud seeding aerosol in a convective feeder cloud are addressed by using radar chaff as a surrogate for aerosol and tracking it with circular-polarization radar. In a case study, a line source of chaff was released by an aircraft at the roots of a growing cloud flanking and feeding into a thunderstorm line. The chaff was tracked as it dispersed in the boundary layer and rose more than 3 km from the cloud base at +14°C to levels cold enough to nucleate ice-forming seeding aerosols. Quantitative measures of the rates of loft and dispersion, and the volume filling and dilution were obtained. The measurements permit examination of the hypotheses and potential efficacy of cloud-base seeding to increase rain and suppress hail. Notably, the problem of delivery, transport, and dispersion of cloud seeding aerosol is much the same as the air quality question of the nature and effect of cloud venting of the boundary layer, and the findings here apply in that context as well.

1. Introduction

Perhaps the most perplexing problem in cloud seeding is that of how to appropriately deliver seeding material to a target cloud. There is ample evidence that seeding aerosol properly placed, timed, and dispersed in well-selected clouds will have desired effects on precipitation processes (Reinking and Meitin 1989; American Meteorological Society 1992). Convective clouds by their nature build on air rising through their bases. For precipitation enhancement or hail suppression, one strategy often used is to seed cumulus congestus from cloud base (Boe et al. 1992). The seeding aerosols released there are thought to be ingested by the target clouds, transported upward, and mixed through a significant portion of the cloud volume where aerosol concentrations remain high enough to induce nucleation. The seeding aerosol may be an ice nucleant that is activated only when lifted to sufficiently cold temperatures, such as a chemical complex that incorporates silver iodide or a hygroscopic nucleant, such as sodium chloride, which is receiving renewed interest concerning its use for broadening the droplet spectrum and accelerating coalescence during its entire ascent in an updraft (Cooper et al. 1994; Mather and Terblanche 1994).

Many questions have arisen in this area. After a line release from an aircraft, what is the nature of the source volume and its dispersion? Is the material ingested en

masse, or does it diffuse to provide a persistent source? How efficiently are such aircraft releases of the seeding aerosol ingested into convective systems? Is the aerosol well dispersed throughout seeded cells, as suggested by chaff tracking in an isolated cumulus (Martner et al. 1992), or is it lifted relatively unmixed in narrow plumes, as suggested from some in situ sampling (Stith et al. 1990)? Are nucleants exposed long enough to accumulate water substance in updrafts? Do ice nucleants reach proper temperature levels, and how much time does resulting ice have to nucleate and grow? Are the timing and location of the nucleation pertinent to the seeding hypothesis?

Growing convective clouds that flank maturing thunderstorms are of particular interest in hail suppression. For building cumulus congestus clouds that have sustained updrafts of a few meters per second, appreciable supercooled liquid water, and low ice particle concentrations (less than a few crystals per liter), it is expected that well-timed, well-targeted seeding with ice-forming nuclei will accelerate precipitation development. Isolated cumulus congestus are expected to produce additional precipitation. However, for flanking congestus, of which feeder congestus are a special case, not only is this expected, but a sequence of events is hypothesized that would divert latent heat and mass from the main cell to produce more rain and less hail.

In particular, Boe et al. (1992) have developed and since improved a chain-of-events hypothesis applicable to the convective clouds that develop over the northern Great Plains. The following is a simplified outline.

Conceptually, seeding a convective cell that flanks a mature thunderstorm will induce early transitions to

Corresponding author address: Roger F. Reinking, Environmental Technology Laboratory, NOAA/ERL, R/E/ET6, 325 Broadway, Boulder, CO 80303-3328.

ice, which will in turn release buoyancy in this cell before a merger would make the energy of latent heat available to the main cell. However, the updraft in the seeded cell will remain essentially unchanged, due to the early conversion that in turn will induce early mass loading and rainout. The consequent trajectory lowering and the glaciation from seeding will reduce feeding of supercooled water and hail embryos into the main cell where hydrometeors (including hail) would otherwise grow much larger. A precipitation shaft developing beneath the previously rain-free base of the flanking cell may interfere with inflow to the thunderstorm, reducing the "fuel" supply. The hypothesis combines the concepts of trajectory lowering, beneficial competition, and fuel starvation, with a key focus on early rainout.

Central questions that encompass those noted above are the following. Do some flanking clouds feed water substance and/or ice into the main cells in a thunderstorm (i.e., are they really feeder clouds), and can either true feeder clouds or nonfeeding flanking clouds be properly seeded to support the early rainout hypothesis?

To answer such questions, the 1993 North Dakota Tracer Experiment (NDTE) used tracer techniques to examine ingestion, transport, and dispersion in convective clouds ranging from individual cells to severe thunderstorms with hail (Boe 1994). As part of NDTE, chaff was released at cloud base, midcloud, around cloud perimeters, and at cloud top, and was tracked by its depolarization signature within clouds and ambient clear air by circular-polarization radar to test varied concepts of entrainment and in-cloud mixing in relation to the seeding hypothesis.

This paper presents a NDTE case study of the chaff tracked in a feeder cell from a cloud-base release, which is the main approach employed in North Dakota's operational cloud seeding program. Since the chaff serves as a surrogate for the aerosol, the study is in essence a fundamental one in transport and dispersion by a convective cloud. The results apply equally well to nonseeding aerosols, such as air pollutants. A majority of the questions asked above apply or could readily be rephrased to address cloud venting of pollutants from the boundary layer, and interpretations would need to be altered only to account for differences in the aerosol chemistry (see Martner and Kropfli 1989).

2. Methodology

Microwave chaff fibers are aluminum-coated glass filaments about $25\ \mu\text{m}$ in diameter that can be dispersed in great numbers and are designed to be detected by radar. The detectability is enhanced by cutting the fibers to half the wavelength of the tracking radar to make them resonant dipoles with large radar cross sections. In NDTE, chaff was cut to 1.6 cm as it was released from an aircraft. Such chaff is sufficiently re-

flective that one piece in each 10^5-m^3 volume of air produces an ample radar return of $-16\ \text{dBZ}$ at a 10-km range (Moninger and Kropfli 1987). The chaff was tracked with a National Oceanic and Atmospheric Administration/Environmental Technology Laboratory (NOAA/ETL) X-band (3.2 cm) multiparameter Doppler radar using a technique called TRACIR (tracking air with circular-polarization radar) (Martner and Kropfli 1989; Martner et al. 1992). For NDTE, the radar was located near New Salem, North Dakota, at $46^\circ 46' 01''\text{N}$, $101^\circ 20' 28''\text{W}$, and 666 m MSL.

This radar has a beamwidth of 0.8° and a sensitivity of approximately $-10\ \text{dBZ}$ at 25 km. For NDTE, the range gates were set at 112.5-m increments, which provided spatially continuous, nonoverlapping data along each radial. Upon release from airborne cutters, chaff reflectivities initially peak near $25\ \text{dBZ}$ and then rapidly diminish to small values. However, depolarization rather than reflectivity is used to detect the chaff. The depolarization caused by the chaff fibers allows them to be detected at any orientation with this radar, not only in clear air, but also within clouds that have reflectivities of less than about $30\text{--}35\ \text{dBZ}$. (This limiting reflectivity for TRACIR is a function of source strength, i.e., the chaff cutter.) The chaff signature is measured in terms of the *circular depolarization ratio* (CDR), which, following the convention of Moninger and Kropfli (1987), is defined as

$$\text{CDR} \equiv 10 \log \left(\frac{P_{\text{cross}}}{P_{\text{main}}} \right), \quad (1)$$

where P_{main} represents the power received in the main, copolarized channel and P_{cross} is the power received in the cross-polarized channel. For perfect spheres, $P_{\text{cross}} = 0$, so $\text{CDR} = -\infty$. Theoretically for chaff, $P_{\text{cross}} = P_{\text{main}}$, so $\text{CDR} = 0\ \text{dB}$ in clear air for any orientation of the chaff fibers. In clouds and precipitation, the high CDR value of chaff is diluted by the low CDR values of hydrometeors to a degree that depends on the chaff/hydrometeor relative concentrations and CDR values (Martner and Kropfli 1989). Thus, it becomes relatively more difficult to detect chaff within the cloud as the reflectivity or depolarization (CDR) of the cloud becomes stronger.

In practice, for new cloud cells composed mainly of cloud droplets, $\text{CDR} \approx -40$ to $-30\ \text{dB}$; however, the minimum measureable depolarization with the X-band radar is about $-30\ \text{dB}$, due to channel cross talk. In contrast, generally $2\ \text{dB} \leq \text{CDR} \leq -7\ \text{dB}$ for chaff in clear air to light echo. In more intense cloud echo, chaff is commonly traceable by spatial and temporal continuity for CDR down to $-10\ \text{dB}$ and is sometimes traceable to -14 or $-15\ \text{dB}$. Here, care must be taken in interpretation because $\text{CDR} \approx -20$ to $-15\ \text{dB}$ for large raindrops, and the depolarization may be still greater (less negative) for graupel or hail.

A threshold of $CDR \geq -10$ dB clearly distinguishes chaff location from cloud echo in the case study presented in this paper. This value was used in the analyses that follow to provide most perspectives of the chaff dispersion and to estimate chaff concentration quantitatively. However, a threshold of $CDR \geq -14$ dB was used as the best demarcation of detectable limits of the chaff boundaries, including maximum loft. The $CDR \geq -14$ dB threshold did introduce considerable cloud signal. Use of this very low depolarization threshold is justified only because of the three-dimensional time-space continuity of the chaff signal, which was determined by inspection of the radar imagery.

The area of dispersion will be confined in space and time according to the track of the release aircraft, the horizontal wind, the vertical transport, turbulent mixing, and the settling rate of chaff ($25\text{--}30$ cm s⁻¹, or about 500 m in 30 min, the duration of a usual case study). The settling rate is normally small ($\leq 5\%$) compared to the vertical motion in convective clouds.

Following Moninger and Kropfli (1987), chaff concentration C (thousands of fibers per cubic kilometer) can be calculated from

$$C = 0.001 \times 10^{(3.15+0.1Z_e)}, \quad (2)$$

where Z_e is the reflectivity (more specifically, the equivalent radar reflectivity factor) in dBZ units of the chaff in clear air. For chaff concentrations normally measured, C is most comprehensibly expressed in thousands of fibers per cubic kilometer; therefore, in this paper we define the *fiber concentration unit* as being 1 fcu $\equiv 10^3$ fibers per cubic kilometer. A correction to Eq. (2) can be applied for the added reflectivity of uniform cloud. The calculation for C is made from Z_e only where CDR exceeds the selected threshold (the chaff signature). Where cloud reflectivity gradients are extreme, the calculation requires assumptions regarding the degradation of the chaff CDR due to the cloud. Fortunately, cloud droplet size is commonly small, and reflectivity is often low (≤ 0 dBZ) or even undetectable in formative convective turrets and flanking/feeder cells, in which case this effect is minor. The analyses here include no adjustment to C for cloud reflectivity.

Chaff can advantageously be released simultaneously with seeding material or other in situ tracers such as gaseous sulfur hexafluoride (e.g., Stith et al. 1994, 1995). With an aircraft, Stith et al. (1990) located ice generated by seeding in cumuli by tracking sulfur hexafluoride that was simultaneously released with the seeding material. The experiment presented here used chaff only to simulate the mixing and transport of seeding material. The chaff-release aircraft was guided via real-time tracking from the radar, which also monitored the developing storm. Sector plan position indicator volume scans with 0.5° or 1.0° elevation increments were employed to find and track the chaff.

In this case, chaff was released for 268 s at an altitude just below cloud base, beginning at 1638:28 LDT.

A release in a large circle was desired to place some of the chaff in the updrafts and some for reference upstream of the cloud mass. For the analyses that follow, we define a reference time t_r as being equal to the start time of each volume scan plus 45 s. Scanning was started with the chaff release; therefore, to within 2 s, the reference time of the first volume ($t_r = t_0 = 0$ s) also corresponds to the starting time of the chaff release plus 45 s. This reference time was better than either the starting time of release or the time that the release ended, because chaff ingestion began shortly after the release was started and well before the release was completed. Further, the selected reference time is suitable because the radar volume scans varied in duration; the radar scanned from the ground up to follow the cloud-base release of chaff, and the number of individual sector scans, of 5 or 10 s each, varied. Early scans in the 0.5–3.0-min volumes found the chaff, whereas higher and later scans within each volume monitored storm structure above the chaff. Reference times and key events in sequence for the complete study are presented in Table 1.

3. The experiment and results

a. Overview

A ring of chaff was dispensed from an aircraft at the base of a cloud flanking a thunderstorm line. The line-source release, which served as a surrogate for cloud seeding aerosol, was well positioned to feed into the storm's circulation, which appeared to be mesocyclonic at low levels. The proximity of the storm, and the radar's view of the chaff release and flanking cells made this an excellent case for chaff tracking. The analyses presented below provide quantitative measurements of the rates of loft and dispersion of the chaff, and of the volume filling and dilution below and within a growing cell that merged into the intense echo core of the storm and, therefore, served as a true feeder cell.

Horizontally, at the release or "source" altitude, dispersion was more rapid immediately below the cloud than in the quieter air upwind. The ring of chaff served as a persistent source for a period comparable to the growth stage of a storm cell. Most of the cell in which the chaff was rising produced minimal reflectivity other than that of the chaff; this suggests it was a fresh cloud, in that it had condensed small droplets but had not yet produced precipitation-sized drops and was, therefore, appropriate for seeding. The cell did feed the chaff into the core of the storm. Before the merger, the chaff in transport spent most of its time at temperatures warmer than 0°C . Hygroscopic nucleants would thus have had more opportunity than ice nucleants to be effective in this case. Relative to the source strength, very substantial dilution of the chaff occurred during the lifting. Nevertheless, the chaff was tracked to altitudes some 3 km above the release level, where ice-nucleating seed-

TABLE 1. Reference times for chaff release and radar volume scans.

Scan volume	t^a	t_r^b	δt_r^c (s)	Event
	1638:28			Start 4-min 28-s chaff release near 0.6 km AGL
V01	1638:30–1639:34	1639:15	0	t_0 \equiv estimated start, ingestible chaff; first radar detection of short chaff line
V03	1640:23–1640:52	1641:08	113	Partial chaff ring; chaff top at 1.0 km AGL
	1642:56		221	End chaff release
V06	1642:18–1643:34	1643:03	228	Full ring, dispersion, and loft to 1.6 km AGL
V08	1645:23–1647:04	1643:08	413	Chaff lofting to 2.0 km AGL
V10	1648:57–1651:18	1649:42	632	Continued loft, 3.2 km AGL
V11	1651:27–1654:07	1652:12	777	Near-maximum detectable loft, 3.6 km AGL
V13	1657:01–1700:21	1654:46	936	Temporarily less loft detectable, 3.2 km AGL
V14	1700:41–1703:51	1701:26	1331	Maximum detectable loft, 3.8 km AGL
V17	1707:31–1701:51	1708:16	1741	Source break up, waning loft to 2.0 km AGL

^a Actual time, LDT.

^b Reference time, start of each volume scan plus 45 s, equals start of chaff release plus 47 s.

^c Elapsed time after $t_0 = 1639:15$ LDT; $\delta t_r = t_r - t_0$.

ing agents would activate, and thereafter was lost into heavier echo.

b. The storm and the chaff release

On 27 July 1993, a small line of thunderstorms gradually developed as it passed to the east of the chaff-tracking radar. The line was approximately 5–10 km wide and 25 km long, with minimum detectable echoes near 0 dBZ and core echoes of 45–55 dBZ (Fig. 1a). These echoes extended from the surface to near 4.5 km AGL. The estimated storm propagation was 6.1 m s^{-1} toward 147° ; however, smaller elements circulated more rapidly within and through the storm. Figure 1b shows the radial velocity of the storm motions relative to the radar at 0.6 km AGL. Here, radial motion (relative to the ground) was only 0 to $+6 \text{ m s}^{-1}$ north of $Y \approx +3.0 \text{ km}$, but $+8$ to $+16 \text{ m s}^{-1}$ south of that position of the steepest north–south velocity gradient, where an east–west shear zone was further indicated by a line of relatively large variance in the radial velocity. Furthermore, an acceleration of about 4 m s^{-1} into the storm was indicated between the chaff ring and the storm core. In all, this pattern was evident between the surface and about 2.5 km AGL and, in storm-relative coordinates, is consistent with the circulation of a mesocyclone. The cell of interest was within the southwest part of this rotating circulation and, thus, positioned where flanking cells are expected to be found according to general thunderstorm models and observations.

The chaff release began with the aircraft headed south into a clockwise ring. An oval chaff ring 6–8 km across was released partially in updraft below the base of visible but echo-free cloud on the upwind perimeter of the line and partially in more settled air slightly farther upwind of the line. The release was made over a 4.5-min period, between 1638:28 and 1642:56 LDT. The reference time for the release t_0 is 1639:15 LDT,

for which elapsed time $\delta t_r \equiv 0$ (see section 2 and Table 1). The release altitude was 0.5–0.6 km AGL, approximately 200 or 300 m below cloud base, and 2.1 km below the freezing level. (A nearby 1436 LDT sounding indicated a lifting condensation level, LCL = 0.8 km AGL, or 850 mb, at $+14^\circ\text{C}$; a level of free convection, LFC = 2.0 km AGL, or 729 mb; and a freezing level near 2.7 km AGL, or 670 mb, in an environment with a lifted index, LI = -1.5). The storm and the chaff gradually moved away from the radar within a 20–40-km range during observation. The “treated” cell was on the radar side of the line. At the $30 \pm 5 \text{ km}$ range where key measurements were taken, the sample volume within the 0.8° beam of the radar was approximately $420 \text{ m} \times 420 \text{ m} \times 112.5 \text{ m}$ (0.020 km^3). This situation presented a near-optimal case for high-resolution chaff tracking.

Figures 1a and 1b, respectively, show the initial 10–30-dBZ echo and the 6–10 m s^{-1} radial velocity of the partially completed chaff ring. During this volume scan ($t_r = 1641:08$ LDT, $\delta t_r = 113 \text{ s}$), the beginning of the merger of the chaff with the 0–10-dBZ cloud echo is already evident. The mesocyclonic circulation is made evident in Fig. 1b, as described earlier. Primarily, the chaff release was immediately southwest of the rotational core of the mesocyclone where the chaff was advected eastward in the faster-moving air. Thus, the release appeared to be well positioned to feed into the storm.

Figure 1c shows that at the time of the release the depolarization from the chaff ring was such that $-2 \leq \text{CDR} \leq +2 \text{ dB}$, while the storm itself indicated $-14 \leq \text{CDR} \leq -12 \text{ dB}$ through much of its area below 2 km AGL; very isolated areas of $\text{CDR} \approx -10 \text{ dB}$ were associated with the strong-echo cores. Since these areas of depolarization within the storm did not reach up to the freezing level, very large, oblate raindrops are suggested in these pockets. No hail was reported in the area. Above 2 km, generally $\text{CDR} \leq -14$. The cloud

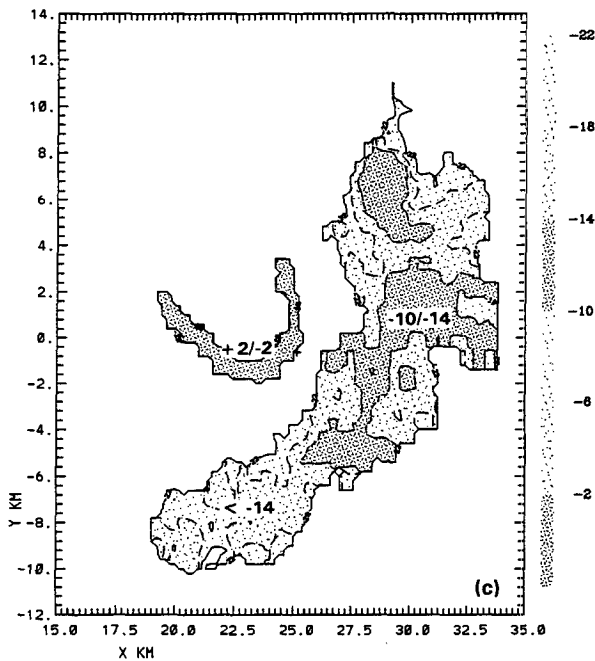
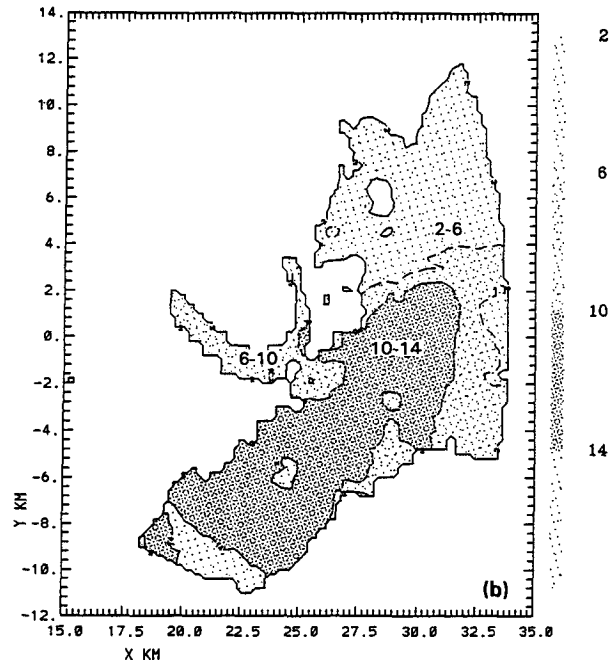
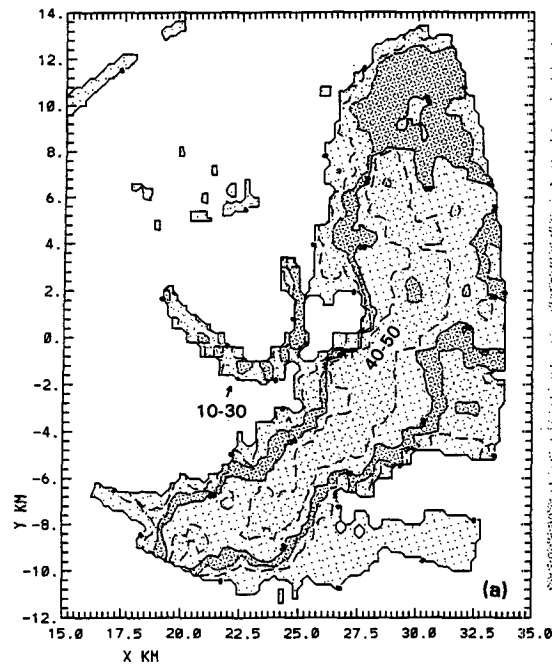


FIG. 1. Observations of the thunderstorm line for 0.6 km AGL (near chaff release level) from a volume scan at 1640:23–1640:52 LDT ($\delta t_r = 113$ s). (a) Radar reflectivity ($Z_e \geq 0$ dBZ), with contour intervals of 10 dBZ (shaded scale, right margin). The horseshoe-shaped echo on the central left flank is that of the chaff during release. (b) Radar-relative velocity ($m s^{-1}$), with contour intervals of $4 m s^{-1}$. (c) Circular depolarization ratio (dB), with contour intervals of 4 dB ($CDR \leq +2$ dB). Distances are measured relative to the radar, which was positioned at $(X, Y) = (0, 0)$; Y increases to the north, X to the east.

depolarization at low altitudes diminished during the next 10 min to $CDR \leq -14$ dB and in small areas to -12 dB.

c. Chaff loft

The chaff release began under the upwind flank of the storm complex on the aircraft's approach to the roots of growing convective cells. The first radar sweep

detected the chaff as a line segment within 6 s after the start of release (Table 1). The portion of the chaff ring dispensed within 2 min after the start of the release tracked under a growing, flanking cell and outward from the storm into the quieter air upwind (Figs. 1a–c; $t_r = 113$ s). Within the ensuing 10–15 min, the chaff was measurably ingested.

Figure 2a shows the three-dimensional structure of the storm for $Z_e \geq -10$ dBZ—that is, all detectable

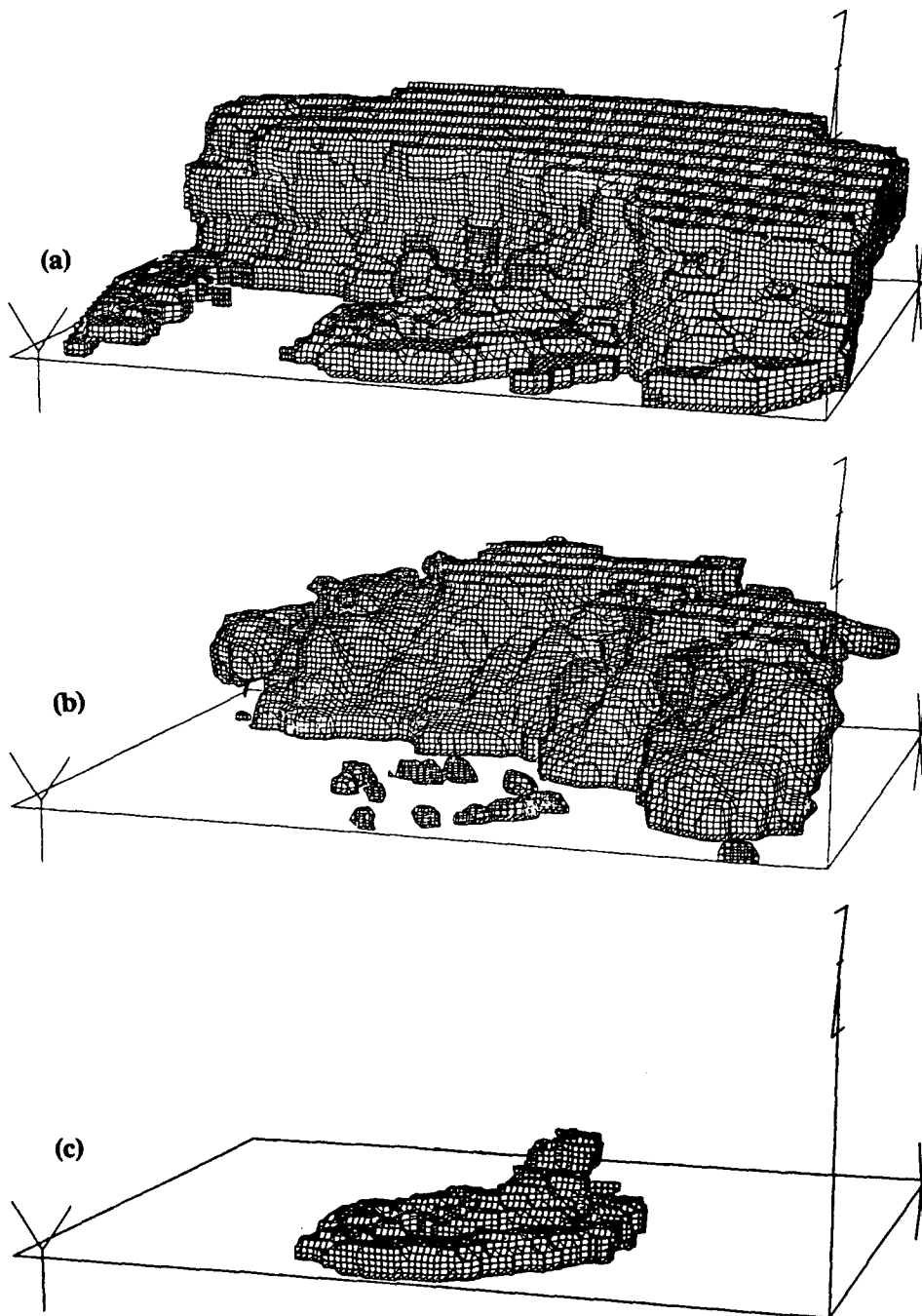


FIG. 2. Three-dimensional perspective of the thunderstorm line from volume scan 11 (Table 1; $\delta t_r = 777$ s). Here, $\delta X = 20$ km, $\delta Y = 26$ km, and $Z = 0$ –10 km AGL. (a) Shows $Z_e \geq -10$ dBZ, (b) $Z_e \geq +20$ dBZ, and (c) $CDR \geq -10$ dB (chaff signature).

echo—from the 1652:12 LDT volume scan ($\delta t_r = 777$ s). The echo in the center foreground is that of chaff partially mixed with and indistinguishable from low-echo cloud. The core of the storm ($Z_e \geq 20$ dBZ) is shown in Fig. 2b. The discontinuous ring in the forefront is chaff echo, most of which was less

than 20 dBZ by this time; no chaff echo was visible at $Z_e \geq 30$ dBZ. Figure 2c shows only the depolarization signature of chaff rising in the flanking cell. This figure documents at least two points: 1) once merger begins, the chaff is indistinguishable from cloud in the reflectivity signal but distinguishable in

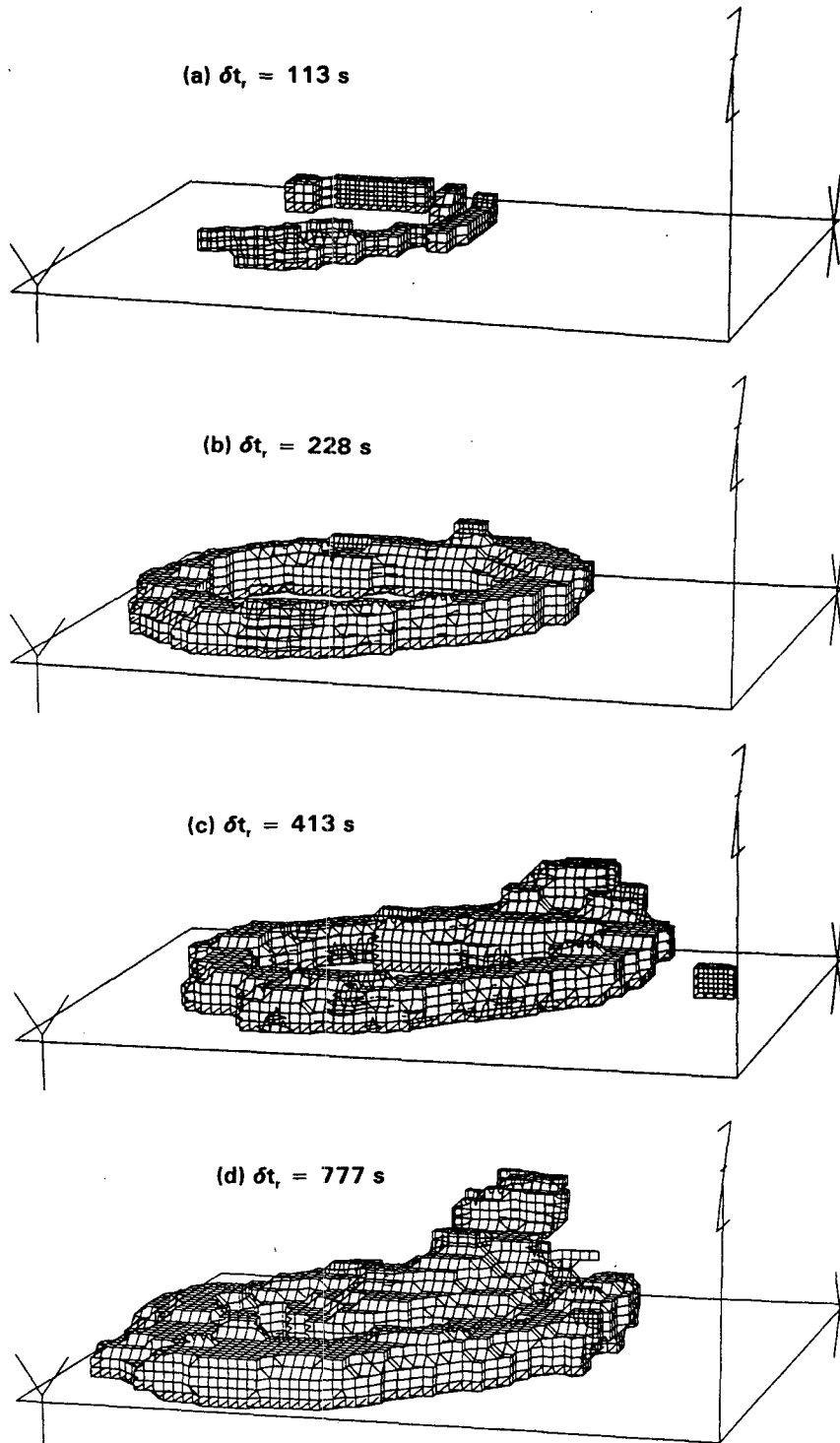


FIG. 3. Chaff ring and rising plume at indicated elapsed times δt , ($C \geq 0$, $\text{CDR} \geq -10 \text{ dB}$; $Z = 0-4 \text{ km AGL}$; $\delta X = 10 \text{ or } 12 \text{ km}$, $\delta Y = 14 \text{ km}$, as in Fig. 6).

CDR; and 2) from a cloud-base release, the chaff can be ingested and substantially lofted by a flanking cloud.

A magnified perspective of dispersion and rise of the chaff is provided in Fig. 3. This shows the chaff (in terms of concentration $C \geq 0$), separated from reflect-

tivity, at indicated elapsed times δt_r , from Table 1. The sequence shows the ring at which time the release was about 60% completed ($\delta t_r = 113$ s; Fig. 3a), followed by initial broadening of the completed ring and the start of ingestion and loft into a cell on the east side of the ring and flanking the storm ($\delta t_r = 228$ s; Fig. 3b). Then, there is considerable loft in a substantially broadened turret of chaff ($\delta t_r = 413$ s; Fig. 3c). Finally, the chaff tower is seen as it appeared near the maximum detectable loft ($\delta t_r = 777$ s; Fig. 3d is the magnified version of Fig. 2c), while indications are that the actual altitude achieved was still higher.

A vertical cross section through the chaff ring and tower, along the 103° radial from the radar and corresponding to Fig. 3d, is presented in Fig. 4a. The com-

parison with the corresponding cross section of the storm reflectivity (with primary chaff echo excluded) in Fig. 4b shows how the tilted chaff turret was feeding into the main cloud mass and area of intense echo, rather than into a separated upwind zone. Thus, it is reasonably clear that the chaff was ingested and lofted by a convective cell that may be described as a feeder cloud. The feeder itself apparently was composed mainly of small droplets because most of it produced no detectable reflectivity; only to the right of $X \approx 32.5$ km in Figs. 4a–c was echo observable, exceeding 0 dBZ.

At this time ($\delta t_r = 777$ s), the detectable chaff reached an altitude of 3.6 km AGL, a significant 3.0 km above the release level. The rise rate of the chaff, approximating the updraft speed, can be determined by

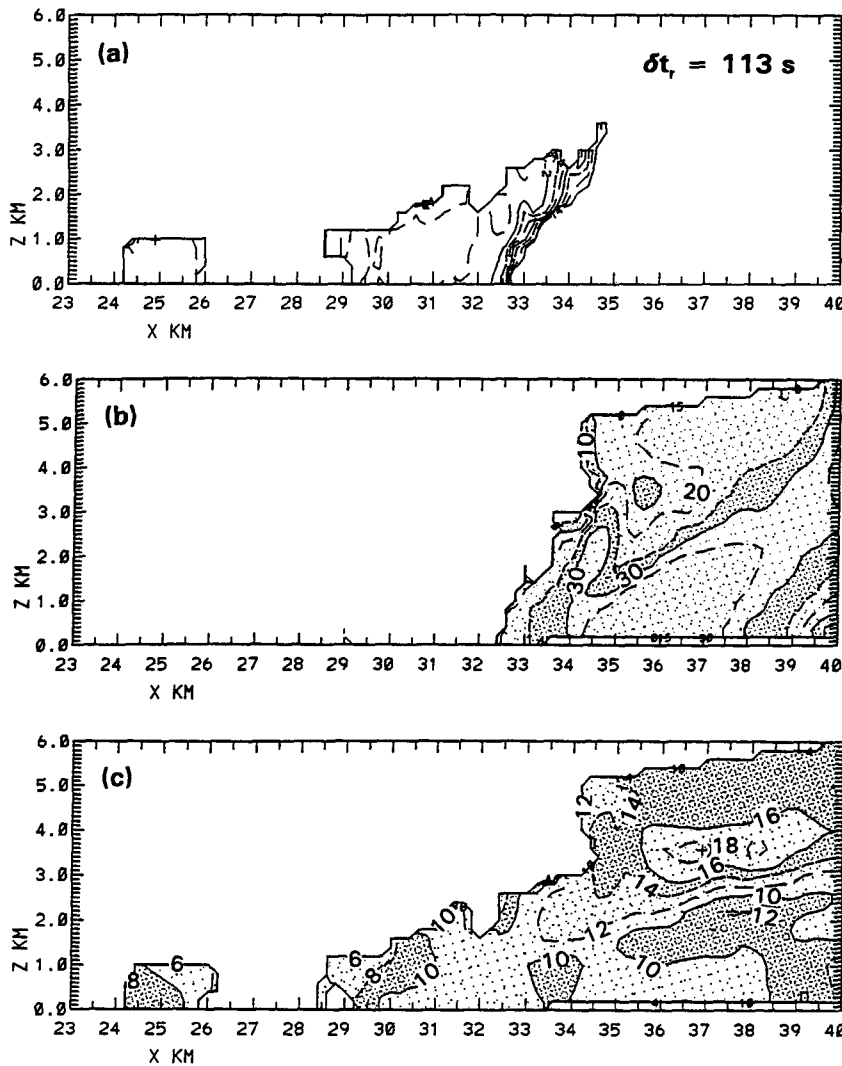


FIG. 4. Vertical cross sections at $\delta t_r = 777$ s of (a) chaff ($CDR \geq -14$ dB), (b) cloud reflectivity (5-dBZ contours, $Z_e \geq 0$ dBZ), and (c) radial velocity, all along the 103° radar radial. Cloud top was higher than the 6 km AGL scan top. In (b), to eliminate primary chaff echo and show cloud echo, reflectivity has been set to zero where $CDR \geq -2$ dB.

following the top of the chaff signature through the sequence of volume scans. Those of Fig. 3 and three subsequent scans at $\delta t_r = 936, 1331,$ and 1741 s are used to map the altitude of highest detectable chaff as a function of time (Fig. 5). The chaff release aircraft had no inertial navigation system but crudely measured a 1.5 m s^{-1} updraft near 0.6 km AGL ; this verified that part of the chaff ring had been released in rising air. The chaff altitude gain observed by radar was continuous and quite steady for the first 13 min, as shown by the rise to the first peak; the rise rate through 3.0 km varied between 2.2 and 5.5 m s^{-1} and averaged 3.9 m s^{-1} . This and other case studies (e.g., Stith et al. 1996) show that the updrafts in feeder cells can be much weaker than those commonly observed in the main cells. After $\delta t_r = 777 \text{ s}$ (13 min), the highest detectable loft wavered slightly and then reached another maximum at 3.8 km AGL at $\delta t_r = 1331 \text{ s}$; loft above 3.2 km AGL was sustained for an additional 13 min after the first maximum altitude of detectable chaff was measured (Fig. 5). Chaff reaching 3.2 km and higher in the cell would not have continued to be detectable without continued renewal; acceleration and advection by the horizontal wind would have carried it into the storm core. Thus, the prolonged detection of chaff loft indicates an updraft sustained for nearly 0.5 h , with corresponding sustained transport of chaff, or equivalently, seeding aerosol, into the main cloud system. After this, the altitude of the highest detectable chaff waned and subsided to 2.0 km at $\delta t_r = 1741 \text{ s}$.

The velocity of the chaff and cloud relative to the radar (Fig. 4c) reveals stretching at low levels. Thus, the western portion of the chaff ring ($X \approx 25 \text{ km}$) was being left behind, while the portion near the storm's edge was moving horizontally with the system. The general increase in velocity with altitude up to about 3.5 km AGL accounts for the tilt of the chaff turret (Fig. 4a) and indicates that as the chaff was lofted, it was accelerated into the main body of the storm.

In summation, the chaff rose more than 3 km in a tilted updraft before the upper reaches of the signature disappeared into the main cloud mass with an echo of $25\text{--}35 \text{ dBZ}$ at the observed juncture (Fig. 4). The transit in cloud took the chaff from $+14^\circ\text{C}$ at cloud base to above the -5°C level of the ambient air. According to the recent calculations by Cooper et al. (1994), 1000 s is ample time for hygroscopic nuclei activated near cloud base to convert a continental droplet spectrum to precipitation. A time period of this order was available in the observed slow but steady updraft of the feeder cell.

The ambient temperature at the highest detected loft, 3.8 km AGL (Fig. 5), was approximately -8°C . The 1436 LDT sounding indicated that adiabatic lifting from cloud base would lead to a 6°C temperature excess of cloud temperature over the environment at the -5°C level. However, the extensive experience from aircraft measurements indicates that the adiabatic loft is nor-

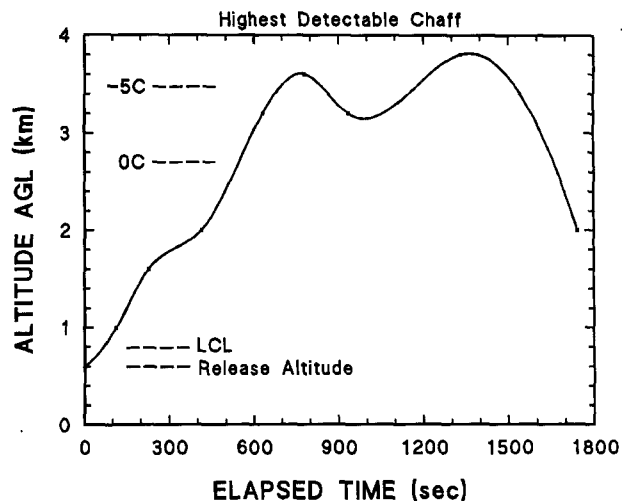


FIG. 5. Altitude of highest detectable chaff as a function of the elapsed time δt_r (spline fit to data points from Table 1). Altitudes of chaff release, lifting condensation level (LCL), freezing level, and -5°C level are indicated (temperatures are those of the ambient sounding).

mally attained only in more protected core cells and that temperatures in feeder cells and small thunderstorms usually exceed the ambient temperature by only 1°C or less. Assuming near-buoyant equilibrium at the top of the feeder cell such that in-cloud temperature did not exceed the ambient temperature by more than 2° or 3°C , then the observed chaff was transported to levels appropriate for ice nucleation by standard seeding agents beginning activation near -4°C . This transport was sustained for 10–15 min.

Together, the continuity of CDR within the updraft, reflectivities that indicate continued updraft and cloud growth above the detectable chaff, and velocity data that show a horizontal component of transport toward the main storm core all suggest that the chaff was lifted to higher and colder altitudes than could be measured. More intense echo or chaff dilution would obscure further detection within the main cloud mass. Stith et al. (1996) report a case in which initial loft of the chaff signature was tracked into but then lost within the intense core of the storm, and a second, gaseous tracer (sulfur hexafluoride) released and transported with the chaff was then found by aircraft and tracked to the upper reaches of the storm (6.5 km AGL). A similar scenario would also have been possible in the present case.

d. Volume filling and dilution

The filling of a significant volume of updraft in the feeder cell is well illustrated by the sequence of Figs. 3a–d. The line source released by the aircraft was initially broadened to about 800 m under the cell, and when first ingested into the turret, the chaff filled only a 300-m-diameter volume as it rose through 1.6 km

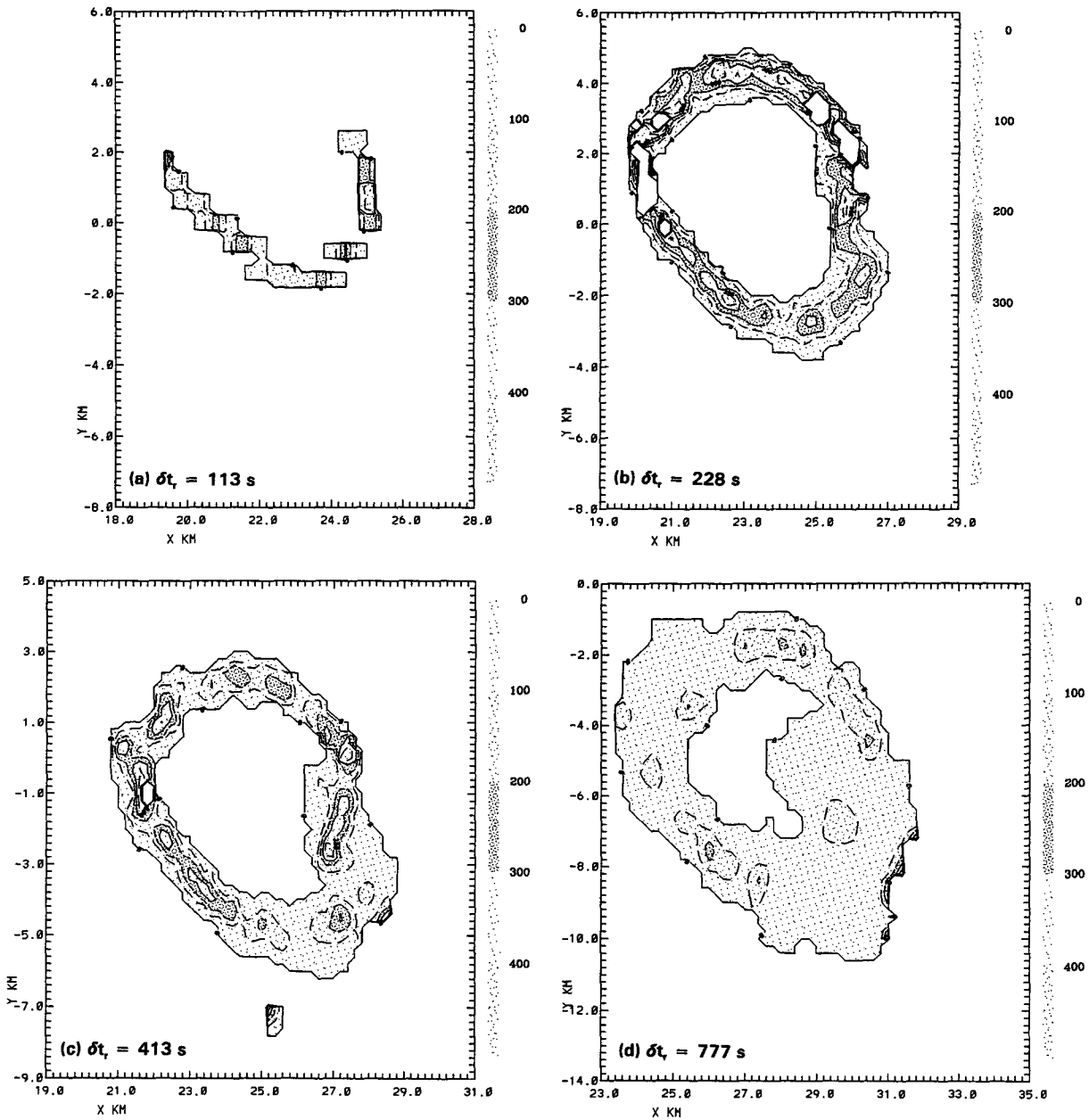


FIG. 6. Chaff concentration [shaded scale, right margin (fcu), from Eq. (2)] at 0.6 km AGL shows spread and persistence of source at release level from $\delta t_r = 0$ s to $\delta t_r = 1741$ s (1639–1708 LDT)—approximately a 0.5-h period.

AGL, 1 km above the release level (Fig. 3b). After 777 s, the roots of the cell, as indicated by the observed chaff, had broadened to some 3.6 km at 1.6 km AGL, and the chaff filled a 2.0-km-diameter core of the cell at 2.6 km AGL (Fig. 4a). Since the cell produced minimal echo and also partly merged with the intense echo of the storm core, we cannot know if the full root system and whole cell volume were filled with chaff; however, these dimensions are consistent with the sizes of new, growing cells and an appropriate factor smaller

than the storm's core cells of some 3–5-km diameter (e.g., Figs. 1a and 4b).

Much of the source pool of chaff at cloud base, including that under the updraft, remained recognizably intact for approximately 25–30 min following the release, referenced to t_0 (Figs. 6a–f). This is simply evidence that not all air moving through the roots of the updraft was entrained into the cloud. The storm moved slowly away from the part of the pool west of the updraft, as the pool stretched in length from about 6 to

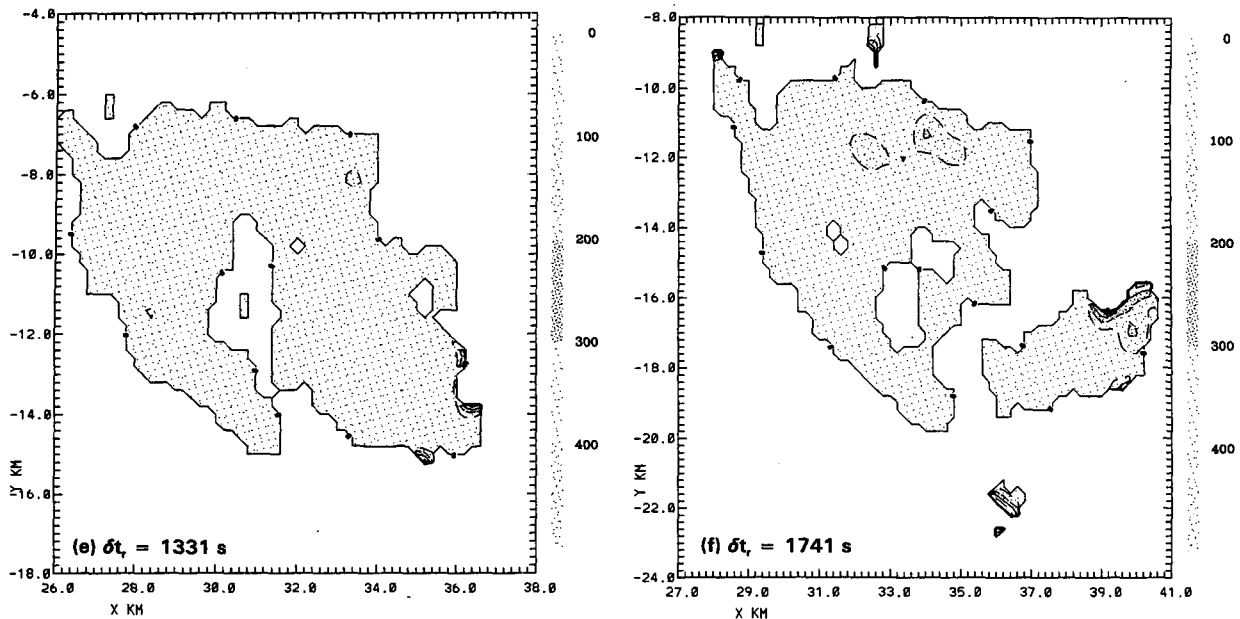


FIG. 6. (Continued)

13 km during the observation period. This stretching and associated diffusion likely contributed to the source pool's persistence outside the cell's main updraft. Continued horizontal entrainment of material from outside the updraft into the roots of the updraft depended on the expanse of the roots, which was not measured.

With $CDR \geq -2$ dB consistently, the pool was easy to track, and the chaff concentrations, total area of the source pool, and dispersion rates at the release altitude could be estimated from the signatures. Area A of the chaff signature and the horizontal dispersion rate $\delta A / \delta t$, determined from Figs. 6a–e, are given in Table 2. The measured area of the source at the 0.6-km release level increased from about 11 to 56 km², a factor of 5, during the first 20 min of dispersion. The horizontal

dispersion rate generally decreased with time from 7.2 km² min⁻¹ initially to 0.6 km² min⁻¹ late in this period. The average was about 3 km² min⁻¹.

The measured radial velocity at the release level was 6–10 m s⁻¹ (Figs. 1b and 4b). Initially, the chaff concentration C [Eq. (2)] at the core of the chaff ring was nominally 100–400 fcu, with peaks of the order of 500 fcu (Figs. 6a,b; $\delta t_r = 113$ and 228 s). As noted earlier, individual chaff fibers will settle only about 500 m in 30 min, so after early fallout of clumps, settling should not confuse the observed dilution. The dispersion and dilution was most rapid in the south and east section of the ring, where the feeder cell drew from the pool; this is particularly evident in Fig. 6c ($\delta t_r = 413$ s) but also indicated in the earlier and later scans. Horizontally, the ring spread about 1.5 times more rapidly under the feeder cloud than in the quieter air upwind.

As the chaff first reached its highest detectable altitude (Fig. 4a), the chaff concentrations at the source level had been reduced to about 200 fcu, or about 50% of the initial source strength, except in some isolated cores (Fig. 6d; $\delta t_r = 777$ s). After another 9 min, only about 100 fcu were detected (Fig. 6e; $\delta t_r = 1331$ s), and significant breakup of the source was under way at $\delta t_r = 1741$ s.

Notably, the chaff source remained intact and continued to be drawn into the feeder cell through most of this half hour, which corresponds to the duration of the lofting above 3.2 km AGL (section 3c). During this period, the reduction rate of source strength was approximately 5% min⁻¹ (referenced to the remaining concentration at the beginning of each successive time interval).

TABLE 2. Horizontal dispersion at chaff release altitude (0.6 km AGL).

δt_r (s)*	δt (s)	A (km ²)	A/A_i **	$\delta A / \delta t$ (km ² min ⁻¹)
113	115	11.0	1.0	7.2
228	185	24.3	2.2	1.8
413	364	29.8	2.7	3.0
777	554	48.3	4.4	0.6
1331		56.3	5.1	

* See Table 1.

** $A_i = 11.0$ km², equals area of partial chaff ring in Fig. 6a multiplied by 1.78 to complete ring (adjustment based on comparison to inner diameter of ring at $t_r = 228$ s).

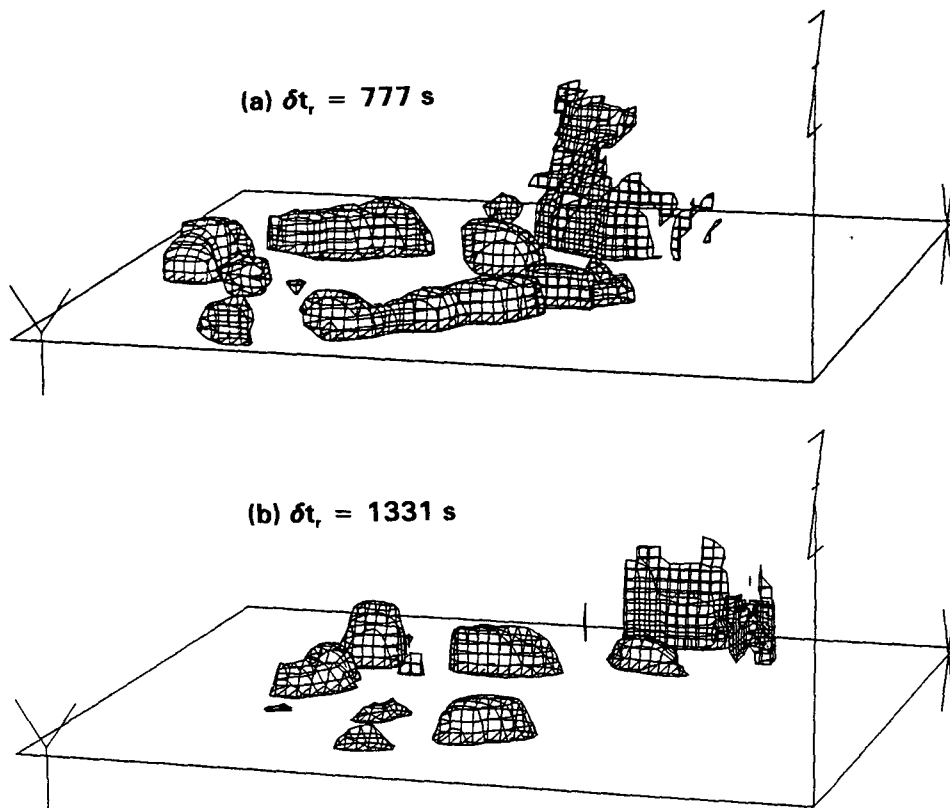


FIG. 7. Volume of chaff with (a) $C \geq 100$ fcu at $\delta t_r = 777$ s and (b) $C \geq 50$ fcu at $\delta t_r = 1331$ s ($CDR \geq -10$ dB).

The dilution of chaff as it was buoyed and mixed upward within the cloud turret can also be estimated. Figure 4a has illustrated the volume of chaff when the maximum altitude in detectable loft was first reached for any fiber concentration exceeding zero. A three-dimensional perspective of the chaff within the same volume, where $C \geq 100$ fcu, is shown in Fig. 7a; this shows that a substantial portion of the chaff fibers were being lofted well up into the turret at this time ($\delta t_r = 777$ s). The chaff at $\delta t_r = 1331$ s for a threshold of $C \geq 50$ fcu is given in Fig. 7b. Here, a similar ring pattern and loft can be noted but for only half the concentration observed 9 min earlier (Fig. 7a).

Vertical profiles of maximum detectable chaff concentration from the south and east sectors of the ring are presented in Fig. 8 for five of the sequential volume scans. The chaff was tracked to successively higher altitudes in this time sequence (see Fig. 5). The decline in source strength with time at 0.6 km AGL follows that in Fig. 6. The vertical profiles represent snapshots in time, so the chaff in the top portions of each profile drew from an earlier and stronger source. All profiles converge to small, albeit measurable, values near 2.0 km AGL that, curiously, correspond to the level of free convection. The chaff first reached 1.6 km (1 km above

release level) around 228 s; by 413 s, the concentration at this reference altitude increased to about 22% of the original source strength (113 s) and then declined to

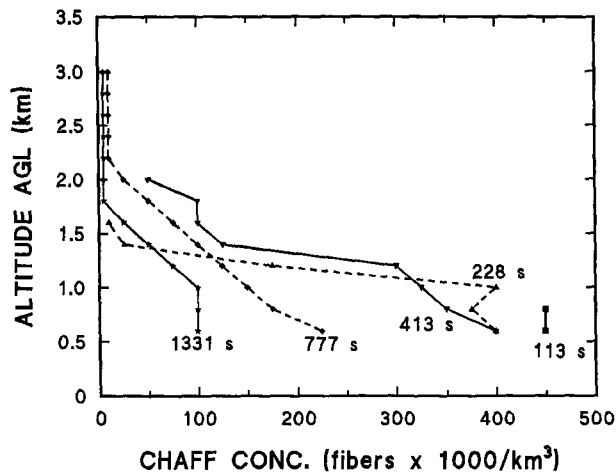


FIG. 8. Maximum detected concentration of chaff C in the portion of the chaff ring where loft occurred, as a function of altitude above ground, from five volume scans at indicated elapsed times δt_r .

17% and 6% in subsequent profiles (Fig. 8). After peaking, this material transported through 1.6 km AGL declined at a rate of approximately $5\% \text{ min}^{-1}$ —that is, at the same rate that the strength of the source at 0.6 km was diminishing.

While the evidence given earlier shows that the source continued to feed the cloud for about 0.5 h, the greatest quantity of material was lofted near the beginning of the period. However, less than 25 fcu, which is 6% of the original source strength and 11% of the concurrent source strength, was measured above 2.2 km (777 s; Fig. 8) when the chaff first reached 3 km above the release altitude (3.6 km AGL; 777 s; Fig. 5). This dilution indicates considerable mixing in nonadiabatic vertical transport, as was assumed in estimating in-cloud nucleation temperatures (section 3c). At face value, this result suggests that for cloud-base releases of equivalent quantities of seeding aerosol, hygroscopic aerosols that affect the cloud immediately after ingestion would have more influence on precipitation than the ice-nucleating aerosols that are activated only after extensive dilution en route to sufficiently cold temperatures. Alternatively, the concentrations of either nucleant at release would need to be adjusted accordingly, or ice-nucleating aerosols might best be released at feeder cell tops.

The caveat surrounding the data in Fig. 8 is that greater concentrations than those measured may have been lofted where the feeder cell merged into intense echo, and chaff could not be detected (Fig. 4b); the profiles presented are those in the portion of the feeder cell that had not merged.

4. Discussion

It is no surprise that growing convective clouds ingest aerosol from cloud base, but the nature of this ingestion, from the roots upward through the volume of individual cells, has not previously been well documented. Many questions concerning the delivery of seeding material, as well as the nature of cloud venting of the boundary layer and the transport of aerosols in clouds to the upper troposphere, need answers. A number of those questions were posed in the introduction. The TRACIR technique is permitting us to find some of the needed answers.

In this case study, an oval line source of chaff was released just below cloud base into the low-level, apparently mesocyclonic, circulation of a small thunderstorm line. The release penetrated the roots of a flanking cell that ingested the chaff. The circular-polarization radar immediately detected the chaff and separated it from low-echo cloud within the storm mass ($Z_e \leq 25\text{--}30 \text{ dBZ}$). The chaff was tracked as it was transported about 3 km vertically from $+14^\circ$ to -8°C ambient. We have classified the flanking cell as a feeder cell because the wind velocity profile and cloud reflectivity structure indicate that the chaff merged into the

intense echo core of the storm. At this merger, the chaff became undetectable, but very possibly rose to much higher altitudes, as in the case discussed by Stith et al. (1996). (The TRACIR technique could be extended to work in stronger cloud reflectivities if the source strength, i.e., the chaff cutter output, could be increased substantially.)

At release level, horizontal dispersion increased the area of the chaff ring by about $3 \text{ km}^2 \text{ min}^{-1}$. This dispersion and associated dilution were most rapid where the ingesting cell drew from the ring. The chaff was not ingested en masse; rather, the source pool persisted and continued to feed the cell for nearly 0.5 h, a period equaling the observed duration of transport of the chaff to highest detectable altitudes. The greatest concentrations of material, however, were ingested and lofted early in this period. A lingering part of the chaff pool in the subcloud layer was left behind as the storm propagated onward.

Judging from the dimensions of the chaff turret, the material appeared to mix through and fill the feeder cell volume. The chaff altitude gain in the cell updraft was continuous and quite steady. An updraft of about 4 m s^{-1} was indicated. This and other cases (e.g., Stith et al. 1995) show that updrafts in feeder cells can be much weaker than in the core cells of thunderstorms, but can also be sustained for the 0.5-h growth period typical of convective cells.

With vertical ingestion and horizontal dispersion, the source strength at release altitude diminished approximately exponentially at a rate of 5% of the remaining material per minute. The concentration of chaff lofted into the cell diminished at approximately the same rate. Although the chaff was efficiently ingested through cloud base, substantial mixing and dilution occurred during ascent; chaff concentrations that were slightly more than 5% of the original source strength, or 10% of the concurrent source strength, were carried through the layer of forced convection and above the LFC (2.0 km AGL).

Cloud-base releases of ice-forming nucleants by aircraft are the main means of delivery in North Dakota's operational hail suppression program (Boe 1992). This experiment, among others during NDTE, showed that chaff (or equivalently, seeding aerosol) from a cloud-base release can be ingested and delivered to desired altitudes and temperatures by a feeder cell, even in systems with only modest vigor.

The high rate of dilution of material observed during ascent, if normal, and the vertical distance between the seeding release and the desired nucleation altitude need to be accounted for when determining appropriate seeding dosages. The $+14^\circ\text{C}$ base of the feeder cell observed in this case study was unusually warm and low for the northern Great Plains climatology, due to the extremely wet 1993 summer season. Thus, the material was forced to transit an unusually deep layer of warm cloud before reaching ice-nucleating levels. Hygro-

scopic seeding aerosols would have nucleated near cloud base with little dilution of concentration and would have then had ample opportunity to broaden the precipitation spectrum in the slow updraft. In this case, hygroscopic aerosols may have offered the best opportunity to mass load the feeder cell updraft, lower precipitation trajectories, and induce premature rainout. To the contrary, ice-forming aerosols would have undergone major dilution before reaching temperatures sufficiently cold to nucleate; once there, winds near the top of the tilted chaff turret suggest that the generated ice would have fed into the core of the storm.

The scenario may be very different for northern Great Plains clouds, which have normal cloud-base temperatures of about +5°C, occasionally colder than 0°C, and rarely warmer than +10°C. Seeding aerosol released at the higher and cooler cloud-base levels would have to transit a much shallower layer and would likely undergo significantly less dilution and less advection into the storm core in reaching the altitudes and temperatures suitable for ice nucleation.

Acknowledgments. This work was funded by the NOAA/North Dakota Atmospheric Modification Program. It was conducted in collaboration with the Atmospheric Resource Board (ARB), State Water Commission, North Dakota, which received research funding under NOAA Cooperative Agreements NA27RA0178 and NA47RA0184. Bruce A. Boe (ARB) is acknowledged for his cooperation and leadership of NDTE. Bruce Bartram (NOAA/ETL) was the radar engineer. Brad W. Orr (NOAA/ETL) heavily supported this work as a field scientist and initiated the data processing. Darren Pastore and Michelle Ryan (NOAA/ETL) subsequently processed most of the data. Tony Grainger (University of North Dakota) directed the chaff release aircraft provided by Weather Modification, Inc.

REFERENCES

- American Meteorological Society, 1992: Planned and inadvertent weather modification: A policy statement of the American Meteorological Society as adopted by the Council on 5 January 1992. *Bull. Amer. Meteor. Soc.*, **73**, 331–337.
- Boe, B. A., 1992: Hail suppression in North Dakota. Preprints, *Symp. on Planned and Inadvertent Weather Modification*, Atlanta, GA, Amer. Meteor. Soc., 58–62.
- , 1994: The North Dakota Tracer Experiment: Tracer applications in a cooperative thunderstorm research program. *J. Wea. Mod.*, **26**, 102–112.
- , and Coauthors, 1992: The North Dakota Thunderstorm Project: A cooperative study of High Plains thunderstorms. *Bull. Amer. Meteor. Soc.*, **73**, 145–160.
- Cooper, W. A., R. T. Brintjes, and G. K. Mather, 1994: Some calculations pertaining to hygroscopic seeding with flares. Preprints, *Sixth WMO Conf. on Weather Modification*, Paestum, Italy, World Meteor. Org., 677–680.
- Martner, B. E., and R. A. Kropfli, 1989: TRACIR: A radar technique for observing the exchange of air between clouds and their environment. *Atmos. Environ.*, **23**, 2715–2721.
- , J. D. Marwitz, and R. A. Kropfli, 1992: Radar observations of transport and diffusion in clouds and precipitation using TRACIR. *J. Atmos. Oceanic Technol.*, **9**, 226–241.
- Mather, G. K., and D. Terblanche, 1994: Initial results from cloud seeding experiments using hygroscopic flares. Preprints, *Sixth WMO Conf. on Weather Modification*, Paestum, Italy, World Meteor. Org., 687–690.
- Moninger, W. R., and R. A. Kropfli, 1987: A technique to measure entrainment in cloud by dual-polarization radar and chaff. *J. Atmos. Oceanic Technol.*, **4**, 75–83.
- Reinking, R. F., and R. J. Meitin, 1989: Recent progress and needs in obtaining physical evidence for weather modification potentials and effects. *J. Wea. Mod.*, **21**, 85–93.
- Stith, J. L., A. G. Detwiler, R. F. Reinking, and P. L. Smith, 1990: Investigating transport, mixing, and the formation of ice in cumuli with gaseous tracer techniques. *Atmos. Res.*, **25**, 195–216.
- , J. Scala, R. Reinking, and B. Martner, 1994: Three techniques for studying the transport and dispersion of seeding material. Preprints, *Sixth WMO Conf. on Weather Modification*, Paestum, Italy, World Meteor. Org., 405–408.
- , —, —, and —, 1996: Combined use of three techniques for studying transport and dispersion in cumuli. *J. Appl. Meteor.*, **35**, 1387–1401.